Applied Clay Science 46 (2009) 43–50

Contents lists available at ScienceDirect

Applied Clay Science

journal homepage: www.elsevier.com/locate/clay

Charge location effect on the hydration properties of synthetic saponite and hectorite saturated by Na^+, Ca^{2+} cations: XRD investigation

M.S. Karmous [a,*], H. Ben Rhaiem [a], J.L. Robert [b], B. Lanson [c], A. Ben Haj Amara [a]

[a] Laboratoire de Physique des Matériaux Lamellaires et Nanomatériaux Hybrides (LPMLNMH), Département de physique, Faculté des Sciences de Bizerte, 7021 Zarzouna, Tunisia
[b] Institut de Minéralogie et de Physique des Milieux Condensés (IMPMC), Campus Boucicaut, 140 Rue de Lourmel, 75015 Paris, France
[c] Environmental Geochemistry Group, LGIT, CNRS – Joseph Fourier University, P.O. Box 53, 38041 Grenoble, France

ARTICLE INFO

Article history:
Received 8 January 2009
Received in revised form 7 July 2009
Accepted 13 July 2009
Available online 18 July 2009

Keywords:
Hectorite
Saponite
XRD
Hydration state

ABSTRACT

This paper aims at comparing the effect of charge location on the hydration properties of two trioctahedral synthetic minerals: saponite and hectorite. The samples were characterised by a layer charge of 0.4 charge per half unit cell and were saturated with Na^+ or Ca^{2+}. The hydration behaviour was studied by determining the structural characteristics which were obtained by modelling XRD patterns.
XRD patterns were recorded under controlled relative humidity (RH). The hydrated states of Ca-hectorite were more homogeneous than those of saponite whereas the transition from 1*W* to 2*W* occurred at lower RH rates for saponite than for hectorite. For heterogeneous samples, the 1*W* and 2*W* layers were stacked randomly fashion for hectorite. Na-saponite-0.4 and Ca-saponite-0.4 were made up of types of layer; one water layer (1*W*) and two-water layers (2*W*). The stacking of these layers showed some segregation.

1. Introduction

The expansion characteristics of natural smectites have been examined in detail under various relative humidities (RH) (MacEvan and Wilson, 1984; Moore and Hower, 1986; Iwasaki and Watanabe, 1988; Watanabe and Sato, 1988; Sato et al., 1992). The basal spacing is a function of water layers and increases gradually with increasing RH.

The nature of the interlayer cation, layer charge and its location have been recognized as important factors controlling the swelling properties of smectites.

Changes of layer charge and charge location can affect smectite hydration. Crystalline swelling of 2:1 clay minerals is controlled by the balance between repulsive forces between adjacent 2:1 layers and attractive forces between hydrated interlayer cations and the negatively charged surface of their 2:1 layers (Norrish, 1954; Van Olphen, 1965; Kittrick, 1969a,b; Laird, 1996, 1999). Thus, crystalline swelling is characterised by the amount of layer charge and its location (octahedral vs. tetrahedral).

Several studies investigated dioctahedral smectite hydration properties using XRD technique. Sato et al. (1992), Yamada et al. (1994), Tamura et al. (2000) and among others have determined these properties following the water basal spacing under variable RH, Ferrage et al. (2005a,b, 2007), modelling XRD patterns. They have studied the influence of layer charge and charge location on the hydration properties of montmorillonite and beidellite. The increase of layer charge shifted the transition from 2*W* (two-water layers) to 1*W* (one water layer) and from 1*W* (one water layer) to 0*W* (dehydrated layer) hydration state towards lower RHs. Beidellite samples displayed the coexistence of larger amounts of the different layer types including non-expandable layers and layers which remained monohydrated at high relative humidities. Laird (2006) has studied the influence of layer charge on smectite swelling; an increase in layer charge decreased crystalline swelling (smaller basal spacings) and increased the size and stability of smectite particles. Layer charge has little or no direct effect on double-layer swelling.

This paper reports a characterisation of the hydration properties of two trioctahedral synthetic smectites: a hectorite and saponite with layer charge of 0.4 charges per a half unit cell. These synthetic minerals were chosen because of their remarkable hydration behaviour. The vast majority of the interlayer spaces contains a monolayer of water at RH = 43% and a bilayer at RH = 85%, as shown by neutron and X-ray diffraction measurements (Malikova et al., 2007).

2. Material and methods

Synthetic hectorite and saponite were prepared by hydrothermal synthesis in Morey-type externally heated pressure vessels, internally

* Corresponding author.
E-mail address: karmousssalah@yahoo.fr (M.S. Karmous).

0169-1317/$ – see front matter © 2009 Elsevier B.V. All rights reserved.
doi:10.1016/j.clay.2009.07.007

Table 1
Atomic positions and number of the different cations in the case of the synthetic hectorite.

Atoms	Number	Z_n (Å)
O_1	2	0.000
O_2	1	0.201
O_3	2	2.253
O_4	2	4.311
O_5	1	6.295
O_6	2	6.593
OH_1	1	1.980
OH_2	1	4.280
Si	2	0.588
Si	2	6.042
Mg	2.6	3.315
Li	0.4	3.315

Table 2
Atomic positions and number of the different cations in the case of the synthetic saponite.

Atoms	Number	Z_n (Å)
O_1	2	0.000
O_2	1	0.201
O_3	2	2.253
O_4	2	4.311
O_5	1	6.295
O_6	2	6.593
OH_1	1	1.980
OH_2	1	4.280
Si	1.8	0.588
Si	1.8	6.042
Mg	3	3.315
Al	0.2	0.588
Al	0.2	6.042

coated with a gold tubing, at 400 °C, 1 kbar P(H_2O), for a run duration of 4 weeks. These synthesis were performed from gels of appropriate compositions prepared according to the conventional gelling method (Hamilton and Henderson., 1968), using high grade Na_2CO_3, Li_2CO_3, $Mg(NO_3)_2$, $Al(NO_3)_3$ and tetraethylorthosilicate $(C_2H_5O)_4Si$ as starting reagents. Full details about synthesis and characterisations are described elsewhere (Bergaoui et al., 1995); the starting synthetic material had a structural formula: $[Na_{0.4}][Mg_{2.6}Li_{0.4}][Si_4]O_{10}(OH)_2$, xH_2O for hectorite and $[Na_{0.4}][Mg_3][Si_{3.6}\ Al_{0.4}]O_{10}(OH)_2$, xH_2O for saponite (x is the number of water molecules per half unit cell). Homoionic Ca^{2+} Hectorite and saponites samples were prepared by conventional ion exchange using aqueous solutions of 0.1 M of $CaCl_2$ (this exchange has been made at least three times). The excess of chloride washed with distilled water until $AgNO_3$ test was negative. The solids were deposited on a glass slide to obtain an oriented aggregate. The samples are referred Hect-Na, Hect-Ca, Sap-Na and Sap-Ca.

XRD patterns were recorded using a Brüker D8-advance using Cu-Kα radiation. Data were recorded in the range of 5–35° 2θ with step of 0.02°2θ and a counting time of 80 sec/step under controlled relative humidity (RH).

Experimental XRD patterns were recorded at relative humidity (RH) conditions between 10% and approximately 90%. For each sample, XRD patterns were recorded following the same sequence of RHs, starting first from 35% (room) to 90% and then reducing RH down to 20% and 10%.

Within this range of RH, it is possible to distinguish between the specific hydration behaviour and structural characteristics of each type of layers and then understand the effect of the location and value of the layer charge on these properties. Experimental XRD patterns were compared to calculated patterns to determine the position of the interlayer cations, the number and the position of the water molecules and the stacking thickness.

The structural characteristics along the normal to the layer plan (z) were determined by comparing the experimental X-ray patterns with theoretical ones calculated from structural models (Drits and Tchoubar, 1990; Ben Rhaïem et al., 2000). The method allowed determination of the number and the position of the intercalated cations and water molecules, the layer and stacking thicknesses, the stacking mode along the normal to the layer plane.

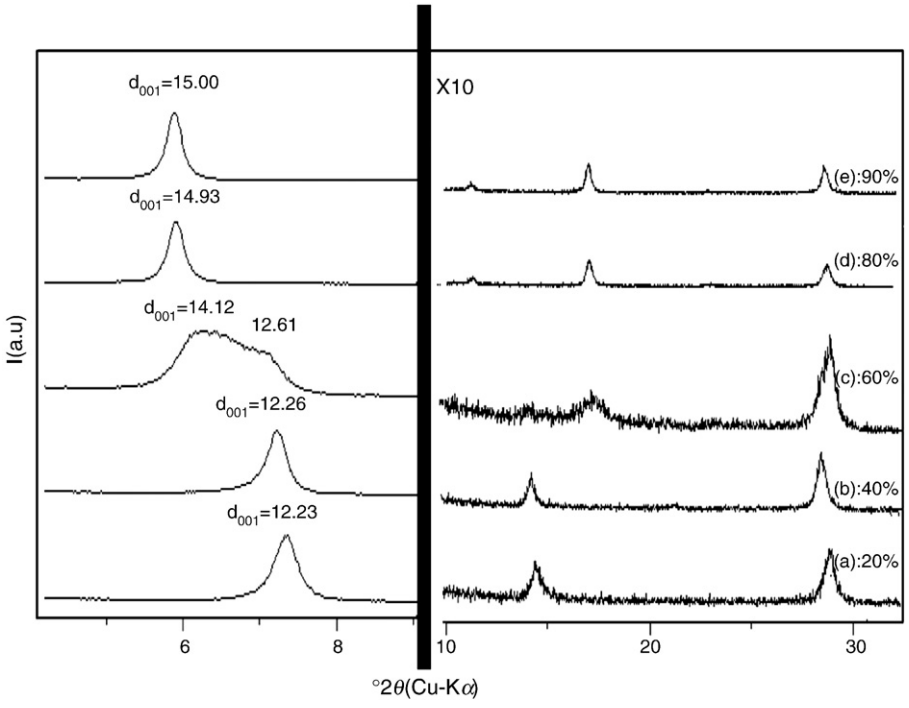

Fig. 1. Experimental patterns of Hect-Na recorded at different RH: (a) 20%, (b) 40%, (c) 60%, (d) 80% and (e) 90%.

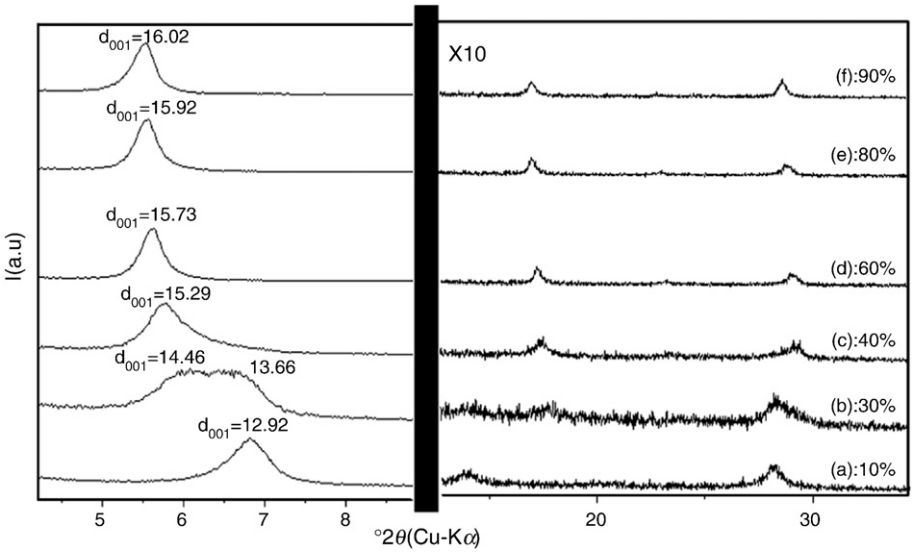

Fig. 2. Experimental patterns of Hect-Ca recorded at different RH: (a) 10%, (b) 30%, (c) 40%, (d) 60%, (e) 80% and (f) 90%.

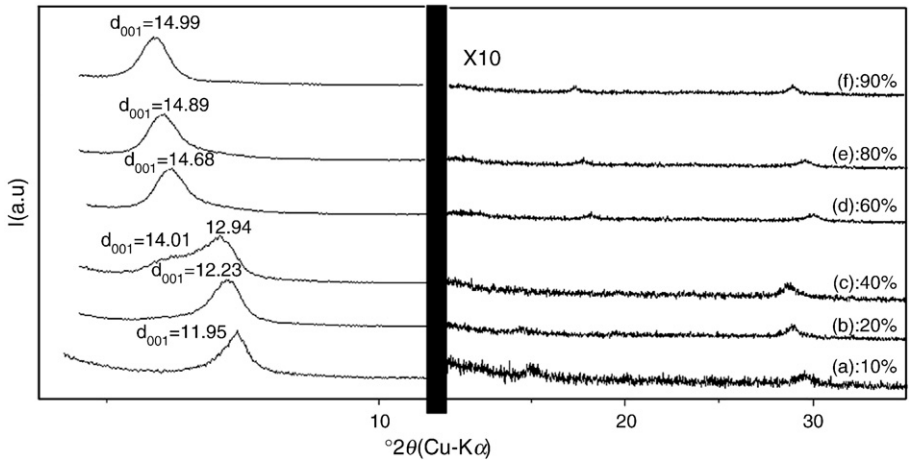

Fig. 3. Experimental patterns of Sap-Na recorded at different RH: (a) 10%, (b) 20%, (c) 40%, (d) 60%, (e) 80% and (f) 90%.

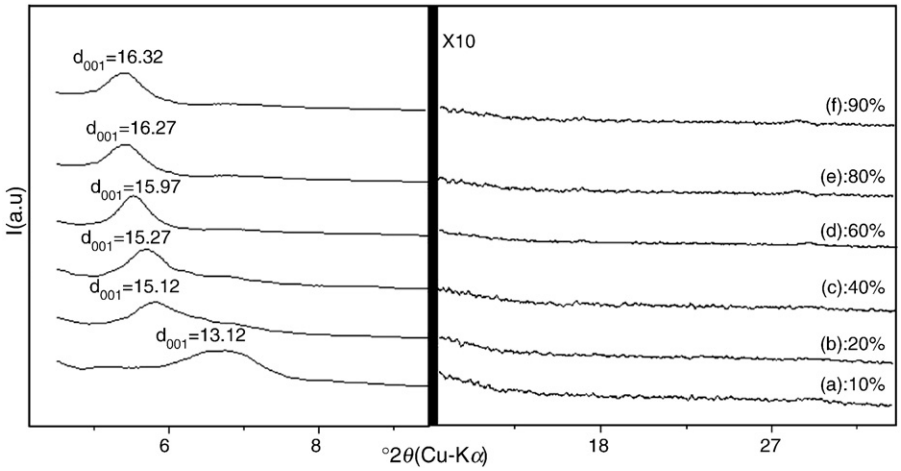

Fig. 4. Experimental patterns of Sap-Ca recorded at different RH: (a) 10%, (b) 20%, (c) 40%, (d) 60%, (e) 80% and (f) 90%.

The atomic coordinates used in the simulation were calculated from Tsipursky and Drits model (1984). In Tables 1 and 2 are given the z coordinates for hectorite and saponite, the origin was taken at the basal oxygen atoms (Karmous et al., 2007). The diffracted intensity for a unit cell along the 00 rod of the reciprocal space is given by the matrix formalism (Drits and Tchoubar, 1990; Ben Rhaïem et al., 1998):

$$I_{00}(2\theta) = L_p \mathrm{Spur}\left(\mathrm{Re}[\phi][W]\left\{[I] + 2\sum_{n}^{M-1}[(M-n)/M][Q]^n\right\}\right)$$

with $L_p = \psi\frac{1+\cos^2 2\theta}{\sin 2\theta}$ (Reynolds, 1986; Ben Haj Amara et al., 1998), where Ψ is the orientation factor of the particles, Re is the real part of the final matrix; Spur, the sum of the diagonal terms of the real matrix; M, the number of layers per stack; n, an integer varying between 1 and $M-1$; [Φ], the structure factor matrix; [I], the unit matrix; [W], the diagonal matrix of the proportions of the different kinds of layers and [Q] the matrix representing the interference phenomena between adjacent layers. For a system made up of two types of layers (A and B) and a nearest neighbour interaction, [Q] takes the form:

$$\det Q = \begin{vmatrix} P_{AA}\exp(-2\pi i s d_A) & P_{AB}\exp(-2\pi i s d_A) \\ P_{BA}\exp(-2\pi i s d_B) & P_{BB}\exp(-2\pi i s d_B) \end{vmatrix}$$

where s is the modulus of the scattering vector; $s = \frac{2\sin\theta}{\lambda}$, d_A and d_B are the d-spacing of layer A and layer B, respectively, and P_{AB} is the conditional probability of passing from a layer A to layer B. The relationship between the different kinds of layer proportions and probabilities are given by (Reynolds, 1980; Drits and Tchoubar, 1990; Pons et al., 1995; Ben Rhaïem et al., 1998):

$$W_A + W_B = 1,\ P_{AA} + P_{AB} = 1,\ P_{BA} + P_{BB} = 1,\ W_A P_{AB} = W_B P_{AB}.$$

During the simulation of the XRD patterns, some corrections must be taken into account (Reynolds, 1986; Ben Haj Amara et al., 1998), such as the Lorentz-Polarisation factor and the preferred orientation.

3. Results

3.1. Qualitative description of the experimental patterns

The hydration state of smectites has been described using three layer types of different layer thickness and corresponding to the most common hydration states reported for smectites in nonsaturated conditions: dehydrated layers (0*W*, layer thickness ~9.6–10.1), monohydrated layers (1*W*, layer thickness ~12.3–12.7), and bi-hydrated layers (2*W*, layer thickness ~15.1–15.8) (Ferrage et al., 2005a,b).

The experimental XRD patterns of, Hect-Na, Hect-Ca, Sap-Na and Sap-Ca recorded at relative humidity between 10 and 90% are shown in Figs. 1–4. The d_{001} and FWHM values were deduced from the position and the full width at half maximum intensity of 001 reflection (Table 3).

Table 3
Basal reflection (position, width) as a function of relative humidity of the Hect-Na and Sap-Na.

Hect-Na			Sap-Na		
HR	d_{001}(Å)	FWHM (°)	HR	d_{001}(Å)	FWHM (°)
20%	12.23	0.326	20%	12.23	0.635
40%	12.26	0.293	40%	12.94–14.01	0.923
60%	14.12–12.61	1.318	60%	14.68	0.599
80%	14.93	0.243	80%	14.89	0.536
90%	15.00	0.234	90%	14.99	0.568

Table 4
Basal reflection (position, width) as a function of relative humidity of the Hect-Ca and Sap-Ca.

Hect-Ca			Sap-Ca		
HR	d_{001} (Å)	FWHM (°)	HR	d_{001} (Å)	FWHM (°)
10%	12.92	0.533	10%	13.12	1.107
30%	14.46–13.66	1.293	20%	15.12	0.769
40%	15.29	0.534	40%	15.	0.555
60%	15.73	0.308	60%	15.97	0.449
80%	15.92	0.310	80%	16.27	1.085
90%	16.02	0.313	90%	16.32	1.100

Hect-Na complex was characterised by symmetrical 001 reflections and a d_{001} spacing of 12.23 to 12.26 Å for RH rates ≤40% (Fig. 1a, b). This corresponded to homogeneous hydration with one water layer (1*W*). At 60% RH, the 001 reflection presented two peaks at 12.61 and 14.12 Å indicating transition from 1*W* to 2*W* state (Fig. 1c). When increasing RH, the position of the 001 reflection shifted 14.93 Å and 15 Å corresponded to the 2*W* hydration state (Fig. 1d, e). Sap-Na exhibited 001 reflections compared asymmetrical to Hect-Na indicating a more heterogeneous hydration. The transition from 1*W* to 2*W* occurred at lower RH rates (40%) (Fig. 3a, b).

Hectorite exchanged with Ca was characterised by a 1*W* state for RH ≤ 10% (Fig. 2a). At RH 30%, the 001 reflection presented two maxima at 13.66 and 14.46 Å (Fig. 2b; Table 4) indicating transition from 1*W* to 2*W*, whereas for Sap-Ca this transition has already started at 15% RH (Fig. 4a). For RH ≥ 40% the d_{001} values corresponded to 2*W* for all samples (Fig. 4b, c).

The FWHM of the 001 reflection of saponite was higher than for hectorite indicating lower crystal thickness and more mixed layer character of saponite. This disorder was also observable by the irrational *00l* reflection positions.

3.2. Quantitative analysis

Modelling of XRD patterns allowed us to determine some structural parameters such as abundance, probabilities of each hydration state, number of layers, number and position of water molecules along the z axis. These parameters (Hect-Na and Sap-Na) at different RH are

Table 5
Structural parameters of Hect-Na and Sap-Na.

Samples		Hect-Na			Sap-Na		
RH(%)		20–40	40–60	60–90	20–40	40–60	60–90
0*W*	d_{001}	10.0 Å	–	–	10.0 Å	–	–
	W	0.1	–	–	0.1	–	–
	n_{H2O}	–	–	–	–	–	–
	Z_{H2O}	–	–	–	–	–	–
1*W*	d_{001}	12.5 Å	12.5 Å	12.5 Å	12.33 Å	12.33 Å	12.33 Å
	W	0.9	0.4	0.05	0.9	0.3	0.2
	n_{H2O}	1.6	1.6	1.6	1.6	1.6	1.6
	Z_{H2O}	9.4 Å	9.4 Å	9.4 Å	9.8 Å	9.4 Å	9.4 Å
2*W*	d_{001}	15.2 Å	15.2 Å	15.2 Å	–	15.2 Å	15.2 Å
	W	0	0.6	0.95	–	0.7	0.8
	n_{H2O}	–	3.2	3.2	–	3.2	3.2
	Z_{H2O}	–	15–9 Å	15–9 Å	–	15.2–9 Å	15.2–9 Å
Number of layers		12	5	10	8	7	7
Succession law		Random	Random	Random	Random	Segregated	Segregated

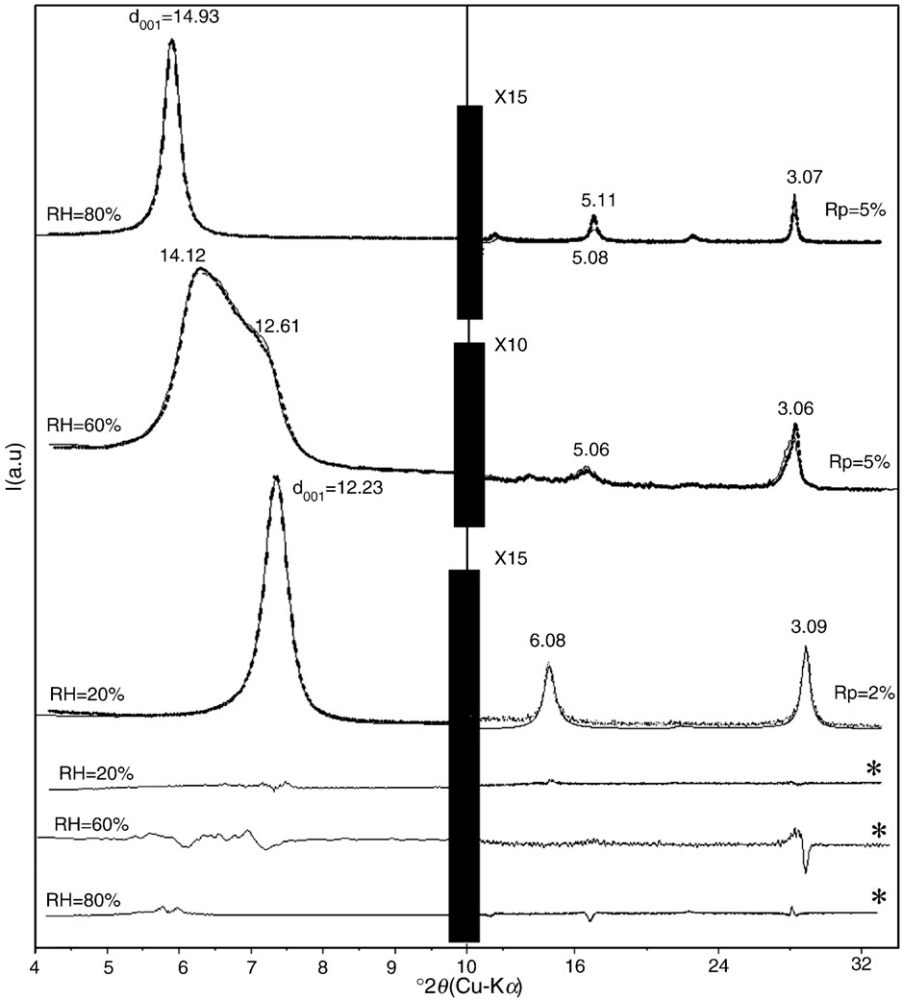

Fig. 5. Best agreement between theoretical (—) and experimental (---) patterns of Hect-Na at RH = 20%, 60% and 80%; (*) represents the difference between theoretical and experimental patterns.

summarised in Table 5. The best agreement between theoretical and experimental XRD patterns is reported in Figs. 5 and 6.

These layers were mainly 1*W* layers in random distribution with small amounts of 0*W* layer. At RH between 40 and 60% the stacking thickness decreased from 12 to 5 layers on average. A transition between 1*W* to 2*W* states took place giving rise to a random mixed-layering of these two hydration states. For higher RH, most layers were 2*W* layers. The stacking thickness increased from 5 to 10 layers on average. The decrease of the mean number of layers per stacking for intermediate RH rates (40–60%) can be attributed to the disorder involved by the interstratification which decreases of the coherent scattering domains. (ii) For Sap-Na, the transition from 1*W* to 2*W* states occurred at lower RH and persist at RH ≥ 20%. We notice the presence of 1*W* state even at 60–90% RH. The mean number of layers per stacking was almost unchanged during the hydration process. The stacking of the two types of layers (1*W* and 2*W*) showed some segregation at RH > 40%, whereas the different types of layers of hectorite were randomly distributed. This can be attributed to the charge location (octahedral or tetrahedral) is entirely octahedral leading to a homogeneous distribution of the tetrahedral sheets.

The structural parameters obtained for the Ca-complexes are given in Table 6 and the best agreement between experimental and calculated XRD patterns is shown in Figs. 7 and 8. Hect-Ca at RH ≤ 30% was constituted of 1*W* layers in majority with small amounts of 2*W* layers. Within 40–60% RH, the stackings were almost homogeneous and made up of 2*W* layers. When increasing RH over 60% we notice the beginning transition from 2*W* to 3*W* hydration states. The mean number of layers per stacking was almost constant and equal to 7. Sap-Ca samples were characterised by mixed-layering between 1*W* and 2*W* layers at all RH. The amount of 2*W* layers increased to the expense of 1*W* layers.

The structure of Sap-Na and Sap-Ca complexes was similar at all RH. Only the distribution of water layer differs. Segregation was observed for RH ≥ 40%. This result indicates the hydration process to be governed by the charge location.

We note that the same results were obtained for dioctahedral smectites, i.e. montmorillonite and beidellite. Ferrage et al. (2007) had demonstrated that beidellite (tetrahedral substitution) presented more heterogeneous hydration state than montmorillonite (octahedral substitution).

4. Conclusion

Hectorite and saponite presented similar hydration behaviour under controlled relative humidity, characterised by a transition between 1*W* to 2*W* layers. Hectorite revealed a high level of homogeneity. The transition to 2*W* layers of saponite was observed at lower RH due to the charge location effect.

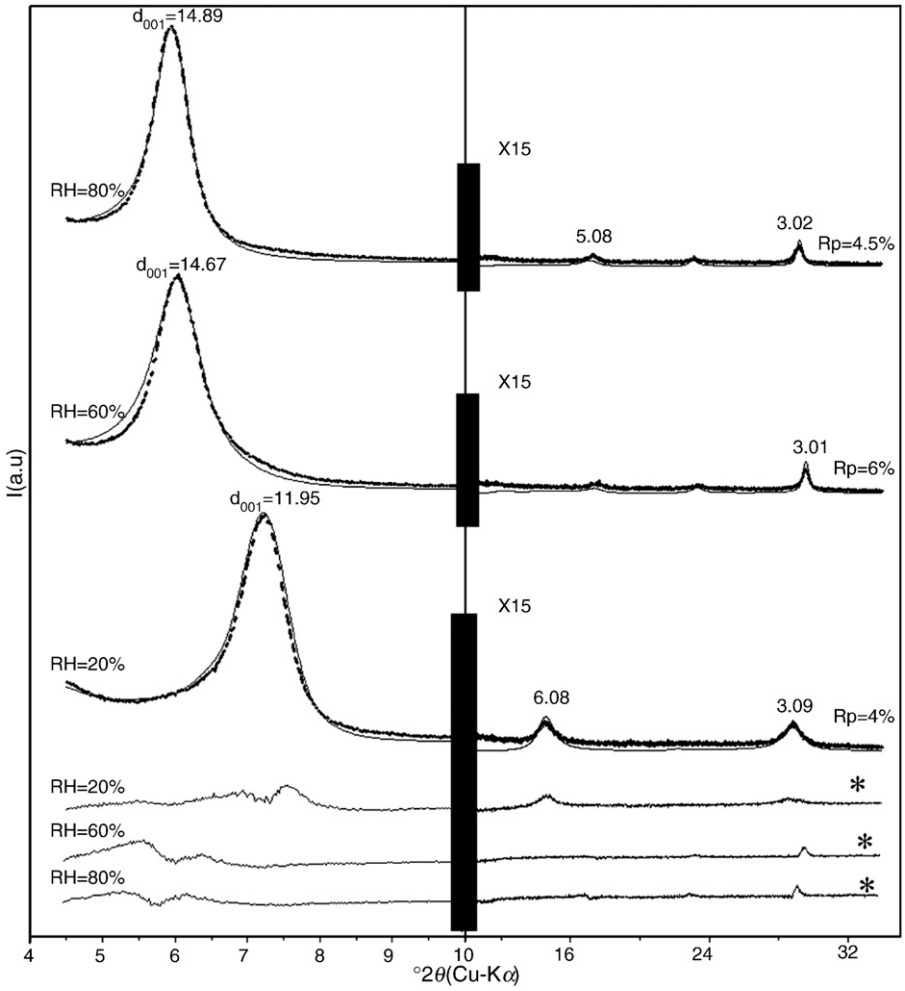

Fig. 6. Best agreement between theoretical (—) and experimental (---) patterns of Sap-Na at RH = 20%, 60% and 80%; (*) represents the difference between theoretical and experimental patterns.

We can conclude that the tetrahedral substitution led to higher hydration heterogeneity. The influence of charge location (tetrahedral vs. octahedral) on the hydration state distribution was pronounced for hectorite and saponite and of minor influence, for dioctahedral smectites montmorillonite and beidellite display the same hydration behaviour as a function of layer charge.

Table 6
Structural parameters of Hect-Ca and Sap-Ca.

Samples		Hect-Ca-0.4			Sap-Ca-0.4		
RH(%)		20–40	40–60	60–90	20–40	40–60	60–90
0*W*	d_{001}	–	–	–	–	–	–
	W	–	–	–	–	–	–
	n_{H2O}	–	–	–	–	–	–
	Z_{H2O}	–	–	–	–	–	–
1*W*	d_{001}	12.6 Å	12.6 Å	–	12.6 Å	12.6 Å	12.6 Å
	W	0.9	0.4	–	0.7	0.2	0.1
	n_{H2O}	2.4	2.4	–	2.4	2.4	2.4
	Z_{H2O}	9.4 Å	9.4 Å	–	9.4 Å	9.4 Å	9.4 Å
2*W*	d_{001}	15.6 Å	15.6 Å	15.6 Å	15.6 Å	15.6 Å	15.6 Å
	W	0.1	0.6	0.85	0.2	0.7	0.8
	n_{H2O}	3.2	3.2	3.2	3.2	3.2	3.2
	Z_{H2O}	15.5–9.6	15.5–9.6	15.5–9.6	15.2–9.6	15.5–9.6	15.5–9.6
3*W*	d_{001}	–	–	18.6 Å	18.6 Å	18.6 Å	18.6 Å
	W	–	–	0.15	0.1	0.1	0.1
	n_{H2O}	–	–	4	4	4	4
	Z_{H2O}	–	–	18–15–12 Å	18–15–12 Å	18–15–12 Å	18–15–12 Å
Number of layers		7	5	7	6	6	8
Succession law		Random	Random	Random	Random	Segregated	Segregated

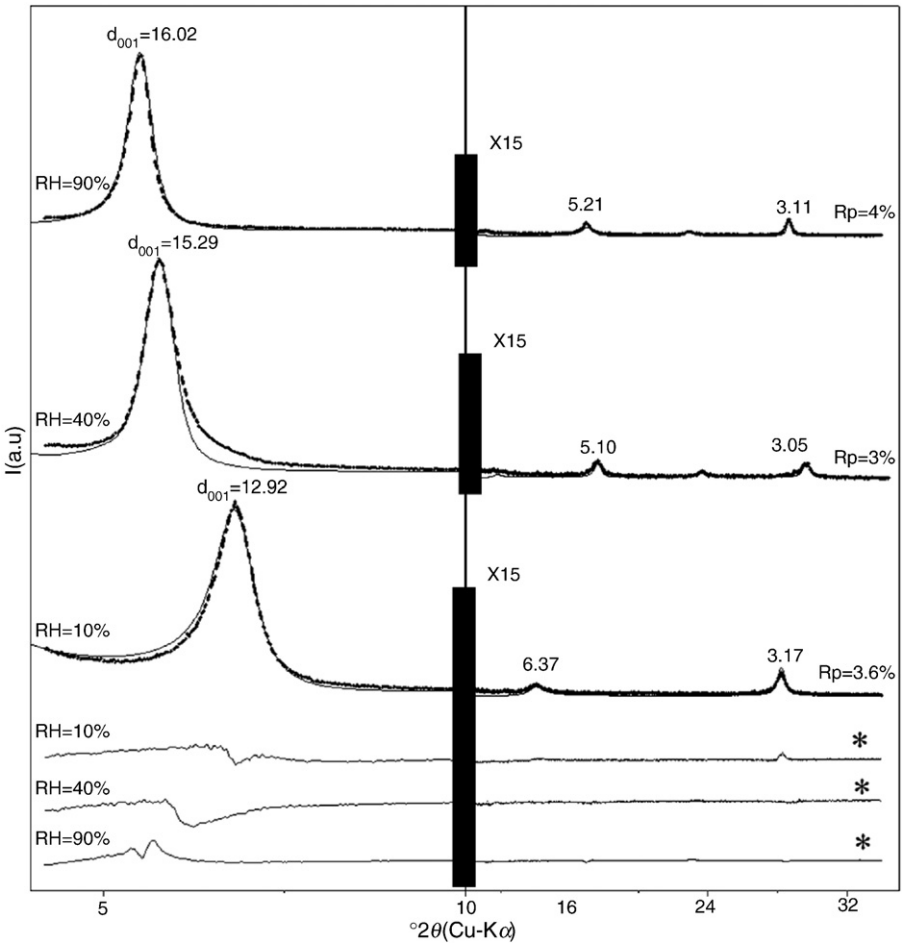

Fig. 7. Best agreement between theoretical (—) and experimental (---) patterns of Hect-Ca at RH = 10%, 40% and 90%; (*) represents the difference between theoretical and experimental patterns.

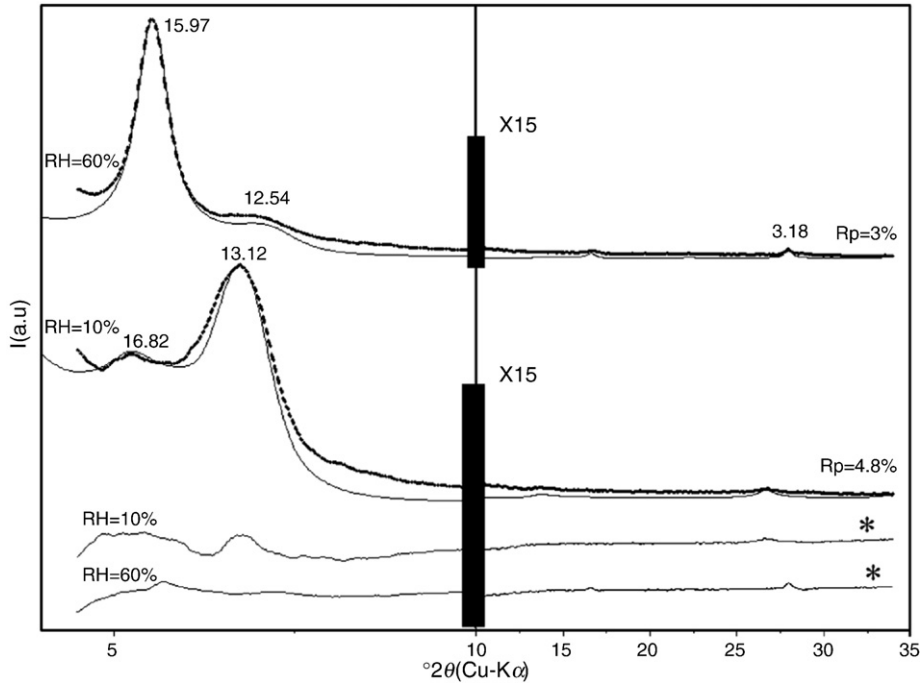

Fig. 8. Best agreement between theoretical (—) and experimental (---) patterns of Sap-Ca at RH = 10% and 60%; (*) represents the difference between theoretical and experimental patterns.

References

Ben Haj Amara, A., Ben Brahim, J., Plançon, A., Ben Rhaïem, H., 1998. Etude par diffraction X des Modes d'Empilement de la Nacrite Hydratée et Deshydratée. J. Appl. Crystallogr. 31, 654–662.

Ben Rhaïem, H., Ben Haj Amara, A., Ben Brahim, J., Ben Brahim, J., 1998. Quantitative analysis of XRD and SAXS patterns: determination of the mineralogy and microstructure of Ca-interstratified clays. Mat. Sci. Forum 278–281, 868–872.

Ben Rhaïem, H., Tessier, D., Ben Haj Amara, A., 2000. Mineralogy of the <2 μm fraction of three mixed-layer clays from southern and central Tunisia. Clay Miner. 35, 375–381.

Bergaoui, L., Lambert, J.F., Frank, R., Suquet, H., Robert, J.L., 1995. Al-pillared saponites: part 3. Effect of parent clay layer charge on the intercalation. Pillaring mechanism and structural properties. J. Chem. Soc., Faraday Trans. 91, 2229–2239.

Drits, V.A., Tchoubar, C., 1990. X-ray Diffraction by Disordered Lamellar Structures: Theory and Application to Microdivided Silicates and Carbons. Springer Verlag, New York.

Ferrage, E., Lanson, B., Malikova, N., Plançon, A., Sakharov, B.A., Drits, V.A., 2005a. News insights in the distribution of interlayer H2O molecules in bi-hydrated smectite from X-ray diffraction profile modeling of 00l reflections. Chem. Mater. 17, 3499–3512.

Ferrage, E., Lanson, B., Sakharov, B.A., Drits, V.A., 2005b. Investigation of smectite hydration properties by modeling experimental X-ray diffraction patterns. Part I. Montmorillonite hydration properties. Am. Mineral. 90, 1358–1374.

Ferrage, E., Lanson, B., Sakharov, B.A., Geoffroy, N., Jacquot, E., Drits, V.A., 2007. Investigation of smectite hydration properties by modeling of X-ray diffraction profiles. Part 2. Influence of layer charge and charge location. Am. Mineral. 92, 1731–1743.

Hamilton, D.L., Henderson, C.M.B., 1968. The preparation of silicate compositions by a gelling method. Mineral. Mag. 36, 832–838.

Iwasaki, T., Watanabe, T., 1988. Distribution of Ca and Na ions in dioctahedral smectites and interstratified dioctahedral mica/smectite. Clays Clay Miner. 36, 73–82.

Karmous, M.S., Oueslati, W., Ben Rhaiem, H., Robert, J.L., Ben Haj Amara, A., 2007. Comparison of hydration properties of synthetic saponite and hectorite saturated by Na^{+}, Ca^{2+} cations. Z. Kristallogr. Suppl. 26, 503–508.

Kittrick, J.A., 1969a. Interlayer forces in montmorillonite and vermiculite. Soil Sci. Soc. Am. J. 33, 217–222.

Kittrick, J.A., 1969b. Quantitative evaluation of the strong-force model for expansion and contraction of vermiculite. Soil Sci. Soc. Am. J. 33, 222–225.

Laird, D.A., 1996. Model for crystalline swelling of 2:1 phyllosilicates. Clays Clay Miner. 44, 553–559.

Laird, D.A., 1999. Layer charge influences on the hydration of expandable 2:1 phyllosilicates. Clays Clay Miner. 47, 630–636.

Laird, D.A., 2006. Influence of layer charge on swelling of smectites. Appl. Clay Sci. 34, 74–87.

MacEvan, D.M.C., Wilson, M.J., 1984. Interlayer and intercalation complexes of clay minerals. In: Rindley, G.W., Brown, G. (Eds.), Crystal Structures of Clay Minerals and Their X-ray Identification. Mineralogical Society, London, pp. 197–248.

Malikova, N., Cadène, A., Dubois, E., Marry, V., Durand-Vidal, S., Turq, P., Breu, J., Longeville, S., Zanotti, J.-M., 2007. Water diffusion by quasi-elastic neutron scattering in a synthetic hectorite—a model clay system. J. Phys. Chem. C 111, 17,603.

Moore, D.M., Hower, J., 1986. Ordered interstratification of dehydrated and hydrated Na-smectite. Clays Clay Miner. 34, 379–384.

Norrish, K., 1954. The swelling of montmorillonite. Discuss. Faraday Soc. 18, 120–133.

Pons, C.H, de la calle, C., de Vidales, M., 1995. Quantification curves for XRD analysis of mixed-layer 14 /10 clay minerals. Clays Clay Miner. 43, 246–254.

Reynolds, R.C., 1980. Interstratified clay minerals. In: Brindley, G.W., Brown, G. (Eds.), Crystal Structures of Clay Minerals and their X-ray Identification. Mineralogical society, London, pp. 294–303.

Reynolds, R.C., 1986. The Lorentz-polarisation factor and preferred orientation in oriented clay aggregates. Clays Clay Miner. 43, 359–367.

Sato, T., Watanabe, T., Otsuka, R., 1992. Effects of layer charge, charge location, and energy change on expansion properties of dioctahedral smectites. Clays Clay Miner. 40, 103–113.

Tamura, K., Yamada, H., Nakazawa, H., 2000. Stepwise hydration of high quality synthetic smectite with various cations. Clays Clay Miner. 48, 400–404.

Tsipursky, S.I., Drits, V.A., 1984. The distribution of octahedral cations in the 2:1 layers of dioctahedral smectites studied by oblique-texture electron diffraction. Clay Miner. 19, 177–193.

Van Olphen, H., 1965. Thermodynamics of interlayer adsorption of water in clays. J. Colloid Sci. 20, 822–837.

Watanabe, T., Sato, T., 1988. Expansion characteristics of montmorillonite and saponite under various relative humidity conditions. Clay Sci. 7, 129–138.

Yamada, H., Nakazawa, H., Hashizume, H., Shimomura, S., Watanabe, T., 1994. Hydration behaviour of Na-smectite crystals synthesised at high pressure and high temperature. Clays Clay Miner. 42, 77–80.